

Meteorological and potential climatic influence on high cyanobacterial biomass within Patos Lagoon (southern Brazil): A case study of the summer of 2019–2020

Beatriz Feltrin Canever^{1*}, Márcio Silva de Souza^{1,2}, Eliana Veleda Klering^{1,2},
Felipe de Lucia Lobo², Elisa Helena Leão Fernandes¹, João Sarkis Yunes¹

¹ Universidade Federal do Rio Grande - Instituto de Oceanografia (Av. Itália, km 8, P.O. Box 474 - Campus Carreiros - Rio Grande-RS, 96203-900 - Brazil)

² Universidade Federal de Pelotas (Pelotas-RS, 96010-610 - Brazil)

* Corresponding author: beatriz.canever@gmail.com

ABSTRACT

Cyanobacterial blooms are a potential threat to human communities and ecosystems. Since the late 1980s, researchers have reported harmful cyanobacterial colonies in Patos Lagoon (PL), the largest coastal lagoon in South America. Most studies concerning harmful blooms in PL have focused on its biology and on its southernmost estuarine region, with little information about its displacement inside the lagoon and the influence of physical forces on its dynamics. This study uses satellite-derived information (normalized difference chlorophyll-a index – NDCI), river discharge data, and meteorological data (wind speed and direction, rainfall, and air temperature) to analyze two bloom episodes in PL, during the austral summer of 2019/2020, specifically in its larger, limnic portion. A 30-year meteorological time series was used to contrast the same summer period. Two remote sensing images from Sentinel-2 were taken of PL margins, near their central portion. The summer of 2019/2020 was drier when compared with the historical data, characterizing low river discharge. This environmental condition was coupled with high temperature, which implies thermal stratification in summer even at 2-m depth sites, which might have promoted cyanobacterial growth and accumulation inside PL. Moreover, weak winds ($<<6 \text{ m s}^{-1}$) seemed to accumulate cyanobacterial patches on the water surface, including after vertical mixing caused by strong winds ($>6 \text{ m s}^{-1}$). The NDCI values represented the two days of blooms, with higher values occurring under higher water temperatures and low wind speeds.

Keywords: Freshwater environment, Wind-driven hydrodynamics, Rainfall, Satellite-Derived biomass index, Climate variation

INTRODUCTION

Since cyanobacterial harmful blooms (cyanoHABs) produce cyanotoxins that can cause skin irritations and cytotoxic effects (Paerl and

Otten, 2013; Paerl, 2017), they are considered an increasing worldwide threat to the environment and to economic and social activities, especially those associated with cultural eutrophication and climate change (Paerl and Huisman, 2009; Kennish and Pearl, 2010; King et al., 2015). These photosynthetic microorganisms usually overgrow after spring (diatom) blooms in many types of aquatic environments, including lakes and lagoons, such as Patos Lagoon (PL) in

Submitted: 05-Nov-2021

Approved: 03-Mar-2023

Associate Editor: Ronald Souza



© 2023 The authors. This is an open access article distributed under the terms of the Creative Commons license.

southern Brazil (Odebrecht et al., 1987, 2005; Haraguchi et al., 2015).

Several studies have been carried out on phytoplankton species in a broader sense, including mostly diatoms, green flagellates, cyanobacteria, and other taxonomic groups, particularly in the estuarine part of PL (Haraguchi et al., 2015, and references therein; Mendes et al., 2017). These and other studies have described the relationship between some biochemical (inorganic nutrients, salinity) and physical factors (temperature, residence time) (Fujita and Odebrecht, 2007) throughout decades (Odebrecht et al., 2010; Haraguchi et al., 2015). Cyanobacteria tend to be noticeable during austral summertime and/or following the decline of more common phytoplankton groups, such as diatoms, within the shallow estuary of PL (Haraguchi et al., 2015 and references therein). Furthermore, the phytoplankton dynamics in this shallow estuary seem to be mainly influenced by wind-driven hydrodynamics on short-term scales (Fujita and Odebrecht, 2007) and by rainfall and drought periods on a seasonal scale (Odebrecht et al., 2010).

However, the major extension of PL is an oligohaline and freshwater system that is still understudied regarding cyanobacteria dynamics. The cyanobacterial dynamics in this limnic system might influence the phytoplankton dynamics farther downstream, to the lower part of PL and its adjacent coastal area (Souza et al., 2018), as seen in other estuaries (e.g., San Francisco Bay estuary, Lehman et al., 2005). The link between the limnic and estuarine parts of PL is mainly due to advection processes caused by continental freshwater contributions and wind forcing (Moller et al., 2001; Möller et al., 2009) on time scales varying from synoptic to interannual (Bitencourt et al., 2020; Távora et al., 2020) since the region is under microtidal influence. In a summertime scenario of weak winds and low discharges establishing stratification, high surface accumulation of cyanobacteria may be a typical biological feature in freshwater bodies (Paerl and Otten, 2013) and the main symptom of the eutrophication process due to rapid cyanobacterial growth in response to elevated concentrations of nutrients (Cloern, 2001; Paerl, 2017).

Particularly around PL estuarine zone, most studies have determined high levels of organic

pollution and inorganic nutrients (such as nitrogen and phosphorus) at sites receiving domestic and industrial wastes close to Rio Grande city (~32°S) (Baumgarten et al., 2001 and references therein; Marreto et al., 2017). To the best of our knowledge, this pattern of nutrient distribution has not yet been fully described across the limnic portion of PL, despite rice culture and cattle stocks possibly being inferred as organic and nutrient sources along both margins of this system (SEMA, 2015; Viégas, 2021). For instance, the quality of the trophic water in certain parts of PL has seldom been determined, being considered hypereutrophic in very shallow embayment (<<1 m in depth) to oligotrophic in deep regions normally encountered at the estuary entrance (Marreto et al., 2017).

Given the potential economic and ecological impacts of cyanoHABs within PL, from its limnic area down to its estuarine region and the adjacent coast, it is essential to understand the relationship between meteorological driving forces and the movements of highly toxic cyanobacterial biomass in the main PL body during the austral summertime. This lack of knowledge is relevant at regional and national scales since the northern and central parts of PL provide agricultural activities, recreational events, and even serve as drinking water sources for population and livestock animals (Yunes, 2009).

Moreover, it has become noticeable that climate change can be responsible for many environmental and ecological alterations (Masson-Delmotte and Zhou, 2021) including the potential of favoring cyanobacterial outbursts and blooms at the expense of other phytoplankton species (Paerl et al., 2016; Paerl, 2017). Some important environmental alterations are related to regime shifts in rainfall and dry cycles worldwide (Paerl et al., 2015 and references therein; Thompson et al., 2015; Masson-Delmotte and Zhou, 2021) and have been reported to alter PL continental discharge contributions and wind regimes (Bitencourt et al., 2020; Távora et al., 2020). For instance, the alternation between flood and drought events can impact the structure and dynamics of cyanobacterial populations, since floods might produce high export rates of nutrients and organic material to adjacent coasts (Souza et al., 2018). On the other hand, dry periods can result

in high phytoplankton biomass (Michalak et al., 2013; Ho and Michalak, 2017) and an increase in residence time (Fernandes et al., 2002; Aguilera et al., 2020), which can promote the development and extension of cyanoHABs in lagoons, such as in the main PL waterbody.

It is difficult, however, to distinguish between the effects of climate change and the eutrophication influence on the occurrence of cyanoHABs and other HABs across different types of waterbodies. One way to achieve this goal is to have a time series of meteorological and biotic information, e.g., phytoplankton biomass and composition. However, in the absence of *in situ* biotic datasets, one can still retrieve information via remote sensing, such as the relative indices of autotrophic biomass, including cyanobacteria (e.g. Mishra and Mishra, 2012; Mishra et al., 2019; Lobo et al., 2021).

Considering the aforementioned information, this work aims to investigate the hypothesis that

dry summer periods, particularly an extremely dry year under a climate change context, enhance the frequency and magnitude of cyanobacterial biomass in the limnic part of PL. The investigation was carried out based on a warm dry period in the austral summer of 2019–2020 that seemed to have promoted high accumulation and growth of cyanobacterial biomass in the limnic part of PL. A meteorological framework and climatological information (1980-2013); Xavier et al., 2016 were related to the biological features based on the normalized difference chlorophyll *a* index (NDCI, see Mishra and Mishra, 2012), considering both margins of the main PL waterbody (Figure 1). It is expected that the results can be an initial assessment of the relationship between meteorological driving forces and cyanoHABs in the limnic area of PL, which will provide valuable information for the establishment of monitoring programs and public policy.

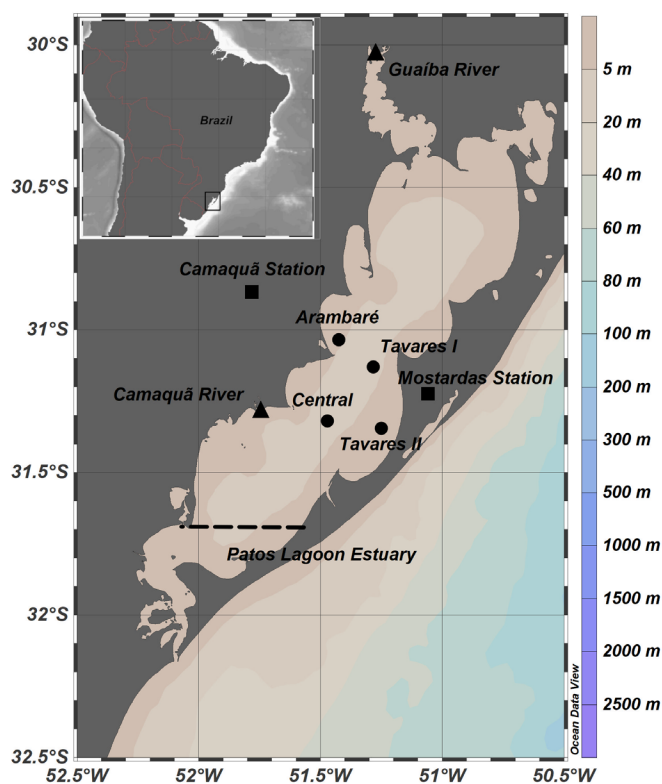


Figure 1. Inset map: Location of Patos Lagoon in southern Brazil. Main map: Depiction of the depth of Patos Lagoon; the four study sites (black circles): Arambaré, Tavares I, Tavares II, and Central; the two main river tributaries (black triangles), Camaquã and Guaíba; and the two meteorological stations (black squares), Camaquã (west) and Mostardas (east). The dashed line delimits the southernmost estuarine portion and the larger limnic portion of the Patos Lagoon.

METHODS

STUDY AREA

The temperate Patos Lagoon (PL) is part of the Patos–Mirim lagoon system and receives waters from a 200,000 km² watershed located between the southern Brazil and the northeastern Uruguay (Seeliger et al., 1998; Odebrecht et al., 2010). PL is the largest lagoonal system in South America (Kjerfve, 1994; Bortolin et al., 2020) and is considered a world natural reserve (Kalikoski and Vasconcellos, 2012). It has one connection with the ocean, in its southern part, and has three main tributaries: Camaquã River, Guaíba River, and São Gonçalo Channel (Figure 1). The region is characterized by its microtidal influence; thus, PL circulation is controlled by winds and freshwater discharges (Moller et al., 2001). During low flow rates (< 2000 m³s⁻¹), wind forcing is responsible for the hydrodynamics in the region (Möller and Castaing, 1999; Távora et al., 2020), otherwise freshwater discharge dominates. Although NE winds and ebbing flows are predominant in summer, this season is also subject to a southern wind influence that favors flood flows towards the estuary, mainly during low river discharge (Möller et al., 2009).

Previous research showed that the El Niño Southern Oscillation (ENSO) is important for PL dynamics and freshwater export to the coast (Möller et al., 2009; Távora et al., 2020). El Niño (La Niña) events imply a higher (lower) rainfall rate, therefore, higher (lower) river discharge in PL. The wind pattern also shifts due to ENSO, with La Niña showing more S-quadrant winds, which can contribute to reducing seaward flow. Because of this low discharge and S-quadrant winds, PL has a higher residence time (Fernandes et al., 2002; Aguilera et al., 2020), which might allow the development of freshwater algae and cyanobacteria, such as *Microcystis aeruginosa* complex (Souza et al., 2018) or *Microcystis* spp., *Spirulina* sp. And *Anabaena* (= *Dolichospermum*) spp. (Ferreira et al., 2004).

METEOROLOGICAL AND CLIMATOLOGY DATA, AND RIVER DISCHARGE

Following casual observations of cyanobacterial blooms next to two cities of the PL (Arambaré and Tavares, west and east of PL, respectively; Figure 2), meteorological data (air temperature, rainfall, and winds) from INMET (National Institute of Meteorology) stations close to Arambaré (Camaquã station) and Tavares (Mostardas station) (Figure 1), were compiled from July 2019 to June 2020. To contrast this time interval of meteorological events with the climatology, a comprehensive meteorological dataset from Xavier et al. (2016) was used. They used air temperature and rainfall data from meteorological station to create an interpolated grid for all regions of Brazil. The grid has a 0.25° interval between each point and has information from 1980 to 2013 for air temperature, and from 1980 to 2015 for rainfall. For this study, information was extracted from unique nodes in the grid to represent four study sites, based on the latitude and longitude: A (Arambaré), TI (Tavares point I), TII (Tavares point II), and C (Central site) (Figure 1). Then, a node located at 31.2900°S, 51.0956°W was selected for rainfall information. This one node was located inside a threshold of 0.50°, encompassing all the four study sites above mentioned and offering the most complete time series dataset. Another selected node (30.05°S and 51.16°W) had a threshold of 1.5°, encompassing those four study sites and corresponding to a larger time series of air temperature. Finally, the monthly accumulated rainfall and the monthly average air temperature were calculated. Recent data on wind speed and direction (from July 2019 to June 2020) were also obtained from the same meteorological stations of Arambaré and Tavares for plotting 3-day, 5-day, and daily wind rose diagrams. Daily river discharge data were obtained from ANA (National Water Agency – <http://www2.ana.gov.br>), from January 2016 to March 2020, for Guaíba and Camaquã Rivers, which are the major tributaries in the northernmost part of PL (Vaz et al., 2011). The graphs were constructed for this time interval, relating them to correspondent NDCI time series.



Figure 2. Photographs of the bloom events: A: in Tavares, December 30th, 2019. B and C: in Arambaré, January 10th, 2020. Source: A. Local citizens, B and C Clic Camaquã (www.cliccamaqua.com.br).

SATELLITE DATA DERIVED (RELATIVE) CHLOROPHYLL-A INDEX, AND ITS RELATIONSHIP WITH WATER TEMPERATURE

The first product to be used was the NDCI (Normalized Difference Chlorophyll-a Index), which is a proxy for phytoplankton biomass derived from Sentinel-2 imagery using Google Earth Engine (Gorelick et al., 2017; Lobo et al., 2021). The Sentinel-2 images were corrected for atmospheric effects based on the SIAC (Sensor Invariant Atmospheric Correction) algorithm

followed by sun glint correction and water mask application (more details according to Yin et al. (2019) and Song et al. (2020)). A cloud mask was also applied to avoid any interference in the analysis. Because of high cloud cover in this region, only a few Sentinel-2 scenes were available for the summer (2019/2020), preventing the acquisition of imagery on the day of both blooms studied. However, a larger time-series investigation was possible due to interpolation of the available data, since most of it (more than 50%) had less than 3 days of missing data.

The same time interval (July 2019 to June 2020) was used to obtain the phytoplankton biomass index NDCI (Mishra and Mishra, 2012), which was derived from Sentinel-2 images. NDCI is based on the use of the red-edge 708 nm and red 665 nm bands combined to evaluate bloom status in the water; and its use is very important when ground truth data are not available (Mishra and Mishra, 2012). For instance, Caballero et al. (2020) highlighted the NDCI potential application to several platforms and diverse environments, producing minimal uncertainty; additionally, bloom status index showed sensibility to chlorophyll-*a* (chl-*a*) concentration in turbid, complex waters (Mishra and Mishra, 2012). Another recent work adopted the threshold of $14 \text{ mg chl-}a \text{ m}^{-3}$ as $\text{NDCI}=0$, with $>20 \text{ mg m}^{-3}$ ($\text{NDCI}=0.06$) as bloom condition in Río de La Plata waters, close to Montevideo, Uruguay (Aubriot et al., 2020). When NDCI equaled to zero, we assumed that chlorophyll-*a* biomass was approximately around 14 mg m^{-3} (Caballero et al., 2020; Lobo et al., 2021). NDCI values higher than zero were associated with bloom conditions, while $\text{NDCI}<0$ did not mean lack of chlorophyll-*a* biomass.

Although there was no *in situ* data to validate the chlorophyll-*a* concentration or the phytoplankton biomass, several publications show that this index is a suitable proxy for this application (Watanabe et al., 2018, 2019). Therefore, the calculated NDCI was adopted to relate with any spatial and temporal, environmental, or meteorological variability. To verify the association between the meteorological and climatological parameters and NDCI, the satellite data were linearly interpolated to a daily interval to augment a temporal coverage description and compensate for the cloud effects and missing data. To consider the daily variation of atmospheric conditions that could be related to the chlorophyll-*a* biomass, the water temperature was retrieved from MODIS (Moderate Resolution Imaging Spectroradiometer)-Terra imagery as follows: Arambaré (31.0349°S , 51.4253°W), Central site (31.3189°S , 51.4725°W), Tavares point I (31.1296°S , 51.2828°W), and Tavares point II (31.3454°S , 51.2499°W). These temperature data

were given as LST (Land Surface Temperature) and were subsequently converted into degrees Celsius.

STATISTICAL ANALYSIS

All the data were expressed as mean \pm SD (standard deviation). To choose between parametric and nonparametric statistical techniques, normality and homogeneity of variances were checked with Kolmogorov–Smirnov and Bartlett tests, respectively (Sokal and Rohlf, 1994). Then, a t-test was applied with the meteorological dataset to contrast their respective means for the INMET stations (from November to March) with the climatological mean according to Xavier et al. (2016)'s dataset. Also, a t-test was applied to the river discharge for a 1980–2018 time-series (National Water Agency: <http://www2.ana.gov.br>) and the time interval from November 2019 to February/March 2020. The statistical significance level accepted was $p<0.05$.

RESULTS

DISTRIBUTION PATTERNS OF AUTOTROPHIC BIOMASS BASED ON NDCI IMAGERY

Typical blue–green cyanoHABs were recorded by local citizens on PL (Figure 2) on December 30th, 2020, and January 10th, 2021. Some spatial and temporal distribution patterns of NDCI values for the main part of PL were seen in the same period. In December 2019, high NDCI values were depicted throughout a few days up to December 31st, especially close to the eastern margin of PL (Figure 3). Following this event, while the eastern margin maintained more patches with a high NDCI, both the NDCI and observational data detected a bloom event on the western margin on January 10th, 2020. We estimate that a high-NDCI event began on January 3rd and lasted for one week. High NDCI values were located northward, mainly near the eastern margin (Figure 3). Generally, considerable high-NDCI patches were also observed at the other sites, such as in the western and estuarine portions of PL.

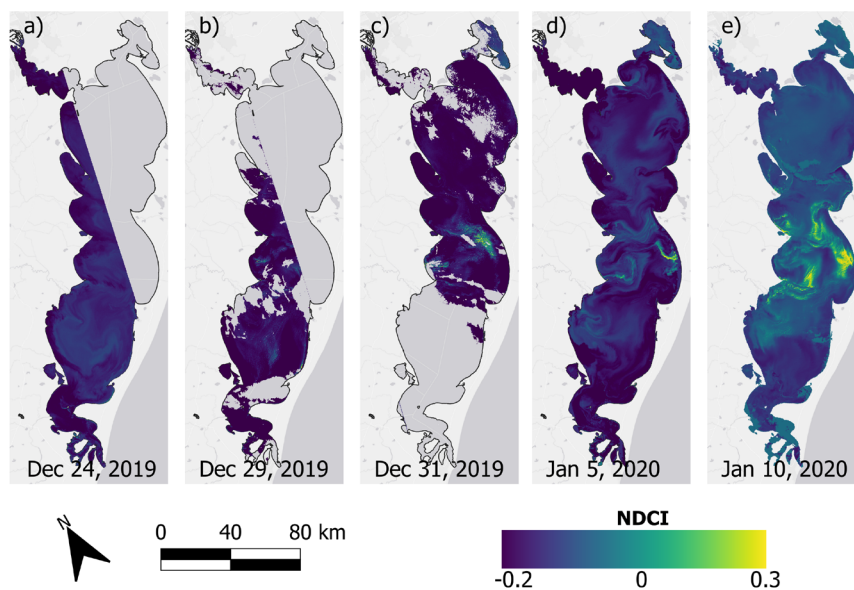


Figure 3. Images of Normalized Difference Chlorophyll-a Index (NDCI) derived from the Sentinel-2 data for the 2019 year: A –24th December, B –29th December, C –31st December (that latter one was a day before the first bloom event observed). Composite images for the whole of Patos Lagoon on 5th January (D) and 10th January (E) 2020, whose the latter day was of a second bloom photographed.

METEOROLOGICAL AND HYDROLOGICAL FEATURES AND RELATIONSHIP WITH NDCI VALUES

Rainfall and air temperature for the austral warmer period (November-December 2019 to January-February 2020) were compared with the monthly mean (\pm standard deviation) rainfall (Table 1) and air temperature (Table 2) in a climatological time series of *circa* 30 years (1980-2013), both for the western margin (Camaquã weather station) and eastern margin (Mostardas weather station) in the main part of PL (Figure 1). Overall, there were significant differences in rainfall only for the eastern margin when compared with the monthly climatology from November to March ($N=5$, $p<0.05$). Nevertheless, both stations showed lower rainfall ($<<80$ mm, on average) than the monthly climatological mean, except for January 2021. However, looking closer at the daily rainfall rates in that month, both stations had higher precipitation precisely on January 10th (Figure 4).

There were slight differences in air temperature between both margins of PL. Low air temperatures

were observed from November 2019 to February 2020 in comparison with the climatological time series ($p<0.05$; Table 2), particularly in January 2020 (24.5 °C). Regarding the local pattern in wind speed and direction (Figure 5a-f), weak winds ($<<6$ m s⁻¹) were observed on bloom days (NDCI $>>0$) on both margins of PL (Figure 5c-f) and were weaker (<4 m s⁻¹) during January 2020 (Figure 5f). Between three and five days before bloom events, strong NE winds (up to 12 m s⁻¹) were prevalent on the eastern margin in December 2019, whereas on the western margin, there was no predominant wind direction in January 2020 (Figure 5a-f). From July 2019 to June 2020, the four sites chosen for describing the relationship between water temperature and NDCI showed higher values only in January 2020, spanning from 0.1 to 0.2 of the NDCI near the eastern margin. This month had a water temperature higher than 20 °C (Figure 6a-d). When comparing the relationship between river discharge and NDCI from January 2016 to March 2020, we noticed that the NDCI was always high in January of every year, particularly in 2018 and 2020, when river discharge was lower than $2,000$ m³ s⁻¹ (Figure 7a-d).

Table 1. Monthly 30-year average rainfall [in mm; from 1980–2015, according to Xavier et al. (2016)] and rainfall data obtained from the Camaquã's and Mostardas' meteorological stations, respectively, during 2019–2020. Note the values in black from November 2019 to February 2020 highlight our summer period studied with cyanobacterial blooms.

Month	30-year average rainfall (mm)		Camaquã's station (mm)		Mostardas' station (mm)	
	Mean	Standard deviation	2019	2020	2019	2020
January	76.5	52.2	139.2	155.6	83.6	85.4
February	88.1	49.0	70.8	35.4	50.4	19.8
March	90.9	59.0	81.2	44.8	-	27.4
April	98.9	62.3	78.6	48.2	-	28.6
May	115.5	69.1	278.4	117.6	-	0.00
June	123.1	65.4	41.2	165.2	47.6	25.2
July	137.8	80.4	179.8		137	
August	114.5	70.1	155		131	
September	133.8	65.1	108.8		103.8	
October	120.5	79.0	127.8		238.2	
November	80.6	56.4	44.6		59.2	
December	85.8	64.5	76.6		19.2	

Table 2. Monthly 30-year mean air temperature [in °C; from 1980–2015, according to Xavier et al. (2016)] and air temperature data obtained from the Camaquã's and Mostardas' meteorological stations, respectively, during June 2019–July 2020.

Month	30-year mean air temperature (+sd; °C)	Camaquã's mean air temperature (+sd; °C) 2019	Camaquã's mean air temperature (+sd; °C) 2020	Mostardas' mean air temperature (+sd; °C) 2019	Mostardas' mean air temperature (+sd; °C) 2020
January	25.56 (5.74)	24.84 (4.27)	23.42 (3.97)	25.90 (2.88)	24.50 (2.44)
February	25.47 (5.56)	23.00 (4.28)	23.05 (4.60)	25.63 (2.54)	23.54 (2.77)
March	24.39 (5.65)	21.40 (4.35)	23.03 (4.42)	26.84 (2.31)	23.76 (1.09)
April	21.26 (5.88)	19.96 (3.75)	18.88 (4.26)	-	20.34 (2.67)
May	17.95 (5.90)	17.47 (3.19)	15.64 (4.73)	-	16.86 (3.47)
June	15.29 (6.14)	16.93 (4.42)	14.77 (4.75)	16.99 (4.51)	15.55 (2.69)
July	14.67 (6.44)	12.24 (4.91)	-	13.24 (3.70)	-
August	16.39 (6.82)	13.71 (5.30)	-	14.30 (3.53)	-
September	17.46 (6.13)	15.05 (4.78)	-	15.51 (2.67)	-
October	20.23 (6.03)	19.26 (5.02)	-	18.75 (2.41)	-
November	22.27 (6.14)	21.30 (4.29)	-	20.98 (2.04)	-
December	24.35 (6.14)	22.98 (5.56)	-	22.58 (3.09)	-

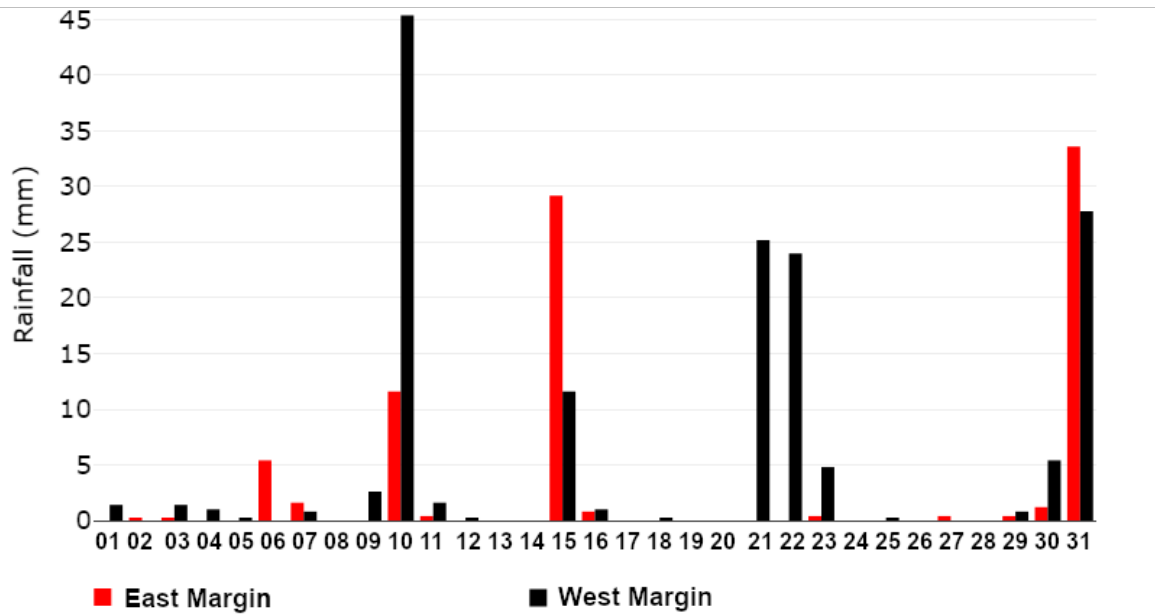


Figure 4. Daily rainfall from the Camaquã's (black) and Mostardas' (red) meteorological stations during January 2020.

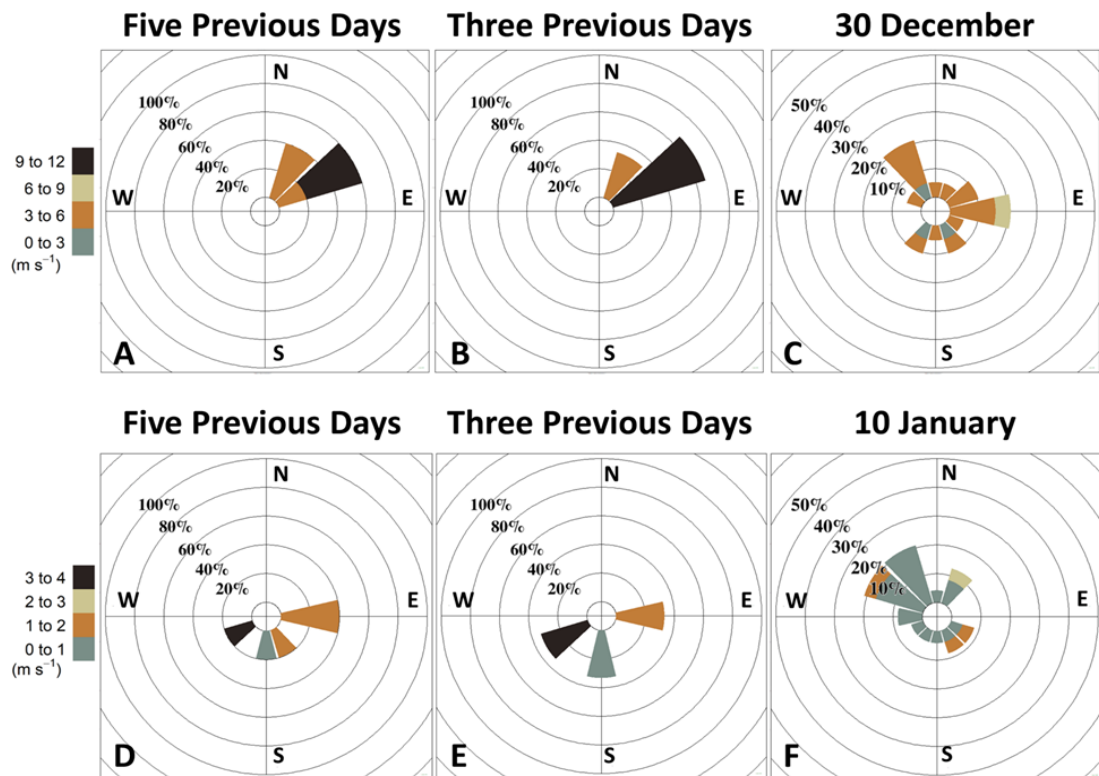


Figure 5. Upper panel: Wind speed and direction from the Mostardas' meteorological station for five days before (A), three days before (B), and on the day of 30th December (C) of bloom. Lower panel: Wind speed and direction from the Camaquã's meteorological station for five days before (A), three days before (B), and on the day of 10th January (C) of bloom. Note that the color range between the upper and lower panel are different due to the significant difference between the wind speed on the east and west margins.

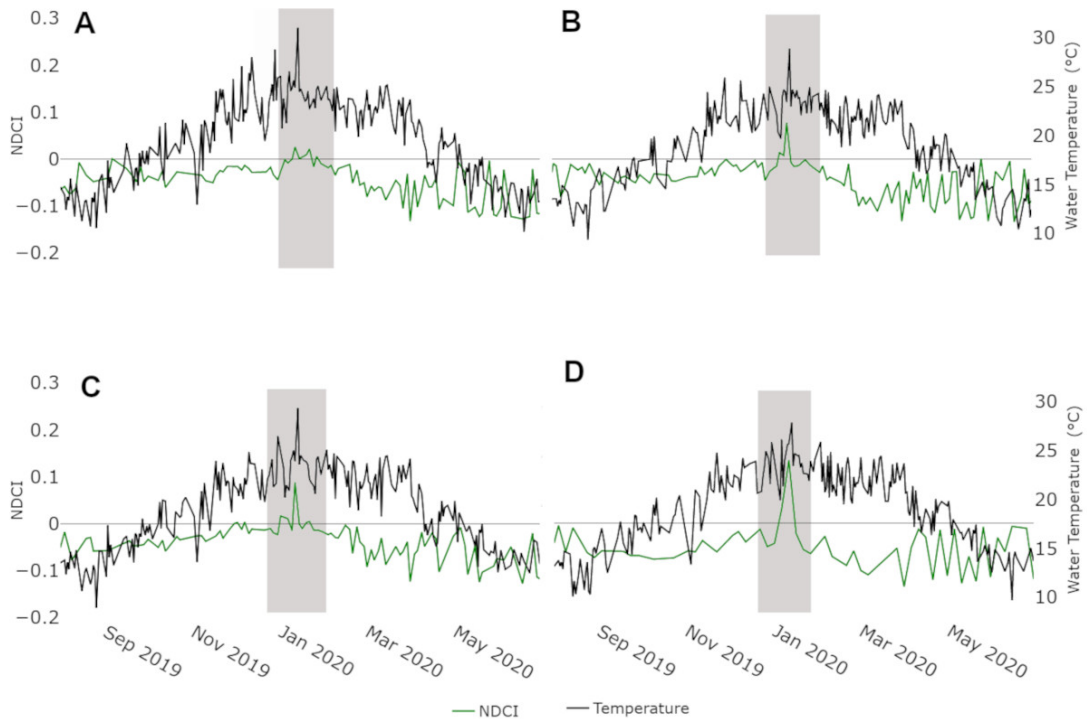


Figure 6. Daily values of NDCI (green lines) and water temperature (black lines) from August 2019 to June 2020, for the study sites of Arambaré (A), Central (B), Tavares I (C), and Tavares II (D), respectively. Note NDCI was derived from the Sentinel-2 data, and the water temperature was retrieved from the MODIS-Aqua. Note that the bold gray line corresponds to 0 on the NDCI scale, therefore, values above this line are associated with bloom conditions. Summer months are highlighted in the gray polygon.

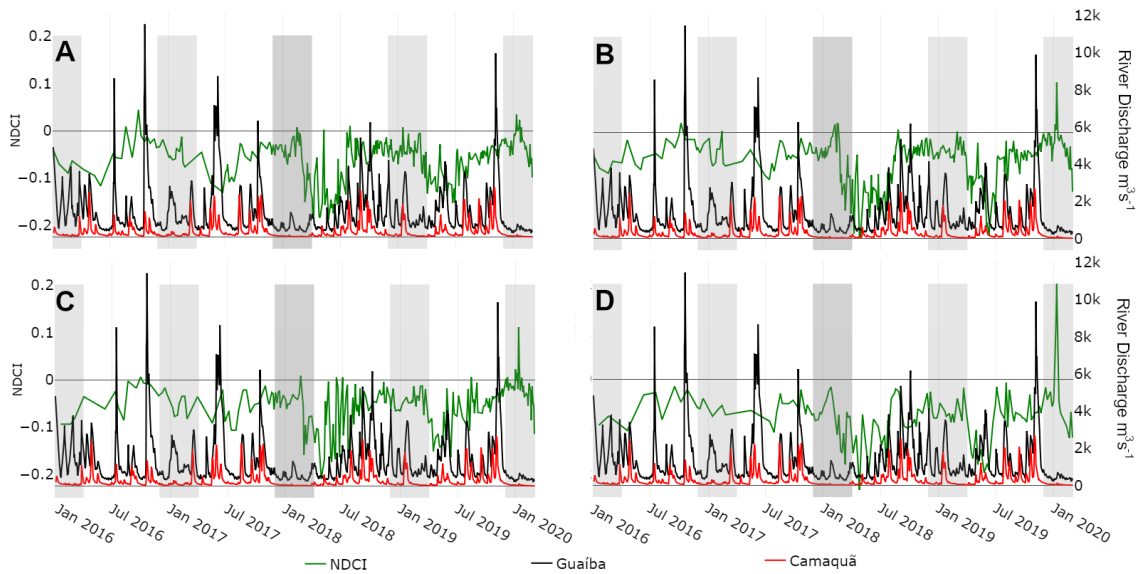


Figure 7. Daily values of NDCI (green lines) for the study sites of Arambaré (A), Central (B), Tavares I (C), and Tavares II (D), respectively, and river discharge data series of Guaíba (black lines) and Camaquã (red lines) from January 2015 to March 2020. Note that the bold gray line corresponds to 0 on the NDCI scale, therefore, values above this line are associated with bloom conditions. Summer months are highlighted in the gray polygon.

DISCUSSION

CYANOHAB THROUGHOUT PL UNDER THE INFLUENCE OF CONTRASTING METEOROLOGICAL EVENTS

We described biological features based on the NDCI during the austral warm period (2019–2020) when cyanobacteria, such as *Microcystis* spp. and *Dolichospermum* spp., tend to be prominent within the PL system (Ferreira et al., 2004; Odebrecht et al., 2005, 2010; Yunes, 2009; Haraguchi et al., 2015). In contrast to all previous studies that concentrated on the estuarine part of PL, the idea behind this work was to relate the NDCI distribution patterns with the meteorological and climatic forces in the large limnic part of PL. Concerning the economic and environmental issues associated with *Microcystis* spp. and *Dolichospermum* spp. in distinct South American bodies of water, the use of NDCI map analysis and *in situ* data showed that, after opening the dam spillways in the Uruguay River and Rio Negro, high cyanobacterial biomass accumulation was observed along the Uruguayan coast in summer 2019 (Aubriot et al., 2020). This occurrence along the Uruguayan coast was attributed to positive precipitation anomalies that were reflected in high flushing of cyanobacterial biomass from upstream sites in the Rio Negro reservoirs (Aubriot et al., 2020).

Previous studies have demonstrated concern about the high frequency and magnitude of cyanoHABs in freshwater systems linked to cultural eutrophication (Carpenter et al., 1998; Reynolds and Davies, 2001) and climate change scenarios (Paerl and Huisman, 2009; Kennish and Pearl, 2010 and references therein; Reichwaldt and Ghadouani, 2012; Paerl and Otten, 2013). In addition, other studies have highlighted the threats of cyanoHABs to ecosystems and social and economic activities (Paerl et al., 2015; Paerl, 2017; Souza et al., 2018). Although no nutrient dataset was available to infer a sign of cultural eutrophication over the NDCI distribution patterns during the studied period, many studies have already shown a high concentration of phosphate (up to $\sim 4 \mu\text{M}$), mostly in the estuarine portion of PL, whereas elevated inorganic

nitrogenous compounds ($10 \mu\text{M}$ of NH_4^+ and up to $70 \mu\text{M}$ of $\text{NO}_2^- + \text{NO}_3^-$) were determined from its limnic portion downward to the estuarine zone (Abreu et al., 1995; Baumgarten et al., 2001; Marreto et al., 2017). Generally, the highest concentrations of all these nutrients were measured close to city margins, associated with anthropic activities: agriculture, livestock farming, industrial production, and urbanized areas (Baumgarten et al., 2001; SEMA, 2015; Viégas, 2021). Thus, we can infer that these nutrient levels could be partly responsible for the high biomass of cyanobacteria in the summertime.

Moreover, it was demonstrated that the summer of 2019–2020 was particularly drier than the climatological normal (Xavier et al., 2016) for the PL region. Low rainfall and river discharge are expected to be reflected in the high retention time of waters. Since Möller Jr. and Castaing (1999) determined some weakly stratified waters, even at shallow sites between 2 and 2.5 m depth, we believe that summer temperatures combined with weakly stratified waters promoted cyanobacterial growth and accumulation throughout the main part of PL. These environmental conditions (low river discharge, high temperatures, and stratified waters) have already been inferred to represent a favorable scenario for the growth of cyanobacteria in lentic portions of the tributaries of the Paraná River, in South America (Devercelli and O'Farrell, 2013). Since some studies have associated cyanobacterial prominence with a lower flushing time and decreasing dilution (Devercelli, 2009; Devercelli and O'Farrell, 2013), we can suggest a similar environmental framework in the middle part of PL in the 2019–2020 summer, although we did not identify or quantify any cyanobacterial species through microscope analysis.

Nonetheless, NDCI values $>$ zero were also observed in the estuarine part of PL, which can be indicative of the presence of cyanobacteria, as was observed *in situ* in samples in other summer periods (Yunes et al., 1998; Ferreira et al., 2004; Fujita and Odebrecht, 2007; Haraguchi et al., 2015). Considering the eventual rainfall observed in January 2020 and PL hydrodynamics, cyanobacterial biomass could have been advected from the uppermost parts down to the estuarine

portion of the PL system. Additionally, nutrient and organic matter enrichment derived from anthropic activities in cities along the margins of PL might have promoted a high trophic status in the middle part of PL (Viéguas, 2021) and around the estuarine sites (Baumgarten et al., 2001; Marreto et al., 2017). The high trophic status of waters combined with low river discharge has been considered to favor cyanobacterial growth (Kiss and Ács, 2002). Otherwise, further studies aiming to assess the potential influence of agricultural activities and domestic waste disposal on cyanobacterial dynamics throughout the margins of cities in the middle portion of PL should be considered.

DIFFERENCES BETWEEN THE MARGINS OF PL AND METEOROLOGICAL VARIABILITY

Generally, hydrodynamics induced by wind action and river discharge have been considered the major driving force of the dynamics of primary producers within PL (Fujita and Odebrecht, 2007; Haraguchi et al., 2015; Andrade et al., 2022). Recently, this relationship was clearly described for the narrow channel that connects PL to the Atlantic Ocean, where the most prominent peak was related to microalgal resuspension due to strong inflowing currents associated with southerly winds (Andrade et al., 2022). Another less intense chlorophyll-*a* peak was related to less saline waters, when northerly winds were reflected in seaward flows (Andrade et al., 2022).

Although our study region was located far northward from the estuarine portion of PL, we believe that a similar interaction between the wind-induced hydrodynamics and the NDCI distribution pattern can be found in the middle stretch of PL. Moderate (3.86 m s^{-1}) to weak (0.70 m s^{-1}) winds were observed in the eastern and western parts of PL, respectively, on days with higher NDCI values, which could have favored cyanobacterial growth and accumulation during summer temperatures of $\sim 20^\circ\text{C}$ (e.g. Paerl and Huisman, 2009; Paerl, 2017). Many species of *Microcystis* and *Dolichospermum* are also capable of vertical transport across the water column, which makes them persistent in waterbodies by harvesting light on the surface but descending to

uptake nutrients near a nutricline (Reynolds and Davies, 2001; Paerl, 2017).

On the other hand, three to five days before the high biomass of primary producers, the middle stretch of PL was under strong winds of up to 8.09 m s^{-1} . We suggest that under these strong winds, there was water column mixing and advection of biomass across the whole waterbody, which also made nutrients available from the boundary water column–sediment interface via the desorption process, particularly of phosphates (Baumgarten et al., 2001). Considering that high hourly and daily wind variability is commonplace, it seemed that the wind speed would have to reduce to $1.71\text{--}2.04 \text{ m s}^{-1}$ or lower for the surface accumulation of cyanobacteria across many locations in the PL system. A similar pattern was observed in Lake Winnipeg, where calm winds allowed cyanobacterial accumulation after strong wind-mixing events (Binding et al., 2018).

Furthermore, the western margin bloom event (NDCI ~ 0.1 , close to Arambaré city) was characterized by strong winds from the 3rd quadrant and an average speed of 1.71 m s^{-1} five days before; when analyzing only the three previous days, there was an increase in the average speed (1.71 to 2.04 m s^{-1}) and frequency of SW winds. Given the need for thorough studies about the SW influence on the cyanobacterial dynamics in the middle stretch of PL, we believe that these winds could have resuspended cyanobacterial inocula, increasing their abundance within the water column (see Andrade et al., 2022). Meanwhile, five days before the eastern margin bloom event (NDCI ranging $0.1\text{--}0.2$, near Tavares city), there was a NE wind predominance with a high speed (6.70 m s^{-1}) that was maintained up to three days previously, with even a higher speed (8.09 m s^{-1}). This scenario suggests a distinct spatial distribution pattern in the NDCI regarding hydrodynamics associated with the wind action between the western and eastern margins.

As Bortolin et al. (2020) described the hydrodynamic conditions evolved from predominant winds and morphometry across the Mirim–Patos lagoonal system, it would be more probable to resuspend sediment and, for our study, cyanobacterial inoculum, near the coastal zones with local depths of $<5 \text{ m}$. Considering that our four

chosen sites (Figure 1) were situated further from the margins, we can thus suggest that high NDCI values were attained within relatively deep (>5 m), stratified waters, partly due to the advection process from the eastern margin under NE winds (Central, Tavares I and II sites). However, cyanobacterial growth at these three sites cannot be excluded, considering the environmental (water temperature ~20°C) and meteorological conditions (calm weather) ideal for cyanobacterial predominance (Paerl, 2017).

The average rainfall for this period (November to February), for the past 30 years, was estimated at 331.1 mm, while for the summer of 2019/2020, the average was lower at both *in situ* meteorological stations (western and eastern stations in the middle stretch of PL). An exception was seen for the western margin (Camaquã) rainfall in January 2020 (155.6 mm); otherwise, the remaining months showed lower rainfall values than the average. On the other hand (at the eastern margin), Mostardas values were almost half the average rainfall for the period (183.6 mm compared with 331.1 mm; $p < 0.05$). Thus, the two bloom events were observed before the relatively high rainfall rates in January 2020. The NDCI-indicated bloom, however, may have been diluted by the high precipitation, which was measured after 6 PM (see Figure 4). Consequently, these NDCI values would have also been affected by relatively high river discharge.

Our work is a fair effort to understand the relationship between a noticeably drier summer and cyanobacterial bloom dynamics via the satellite-derived NDCI. A comprehensive review showed that the impact of changes in precipitation patterns tends to be very complex and should strongly depend on the site-specific dynamics, cyanobacterial species composition, and cyanobacterial strain succession (Reichwaldt and Ghadouani, 2012). Larger and more intense precipitation events should mobilize nutrients on the land and increase nutrient enrichment of receiving waters (Paerl and Paul, 2012), but they could also represent high flushing and advection of cyanobacterial biomass toward coastal areas (Reichwaldt and Ghadouani, 2012). However, drier periods implied higher water retention time, promoting local growth and permanence of cyanobacterial biomass (Reichwaldt and

Ghadouani, 2012). Therefore, we can indicate that lower rainfall/river discharge, mainly on the eastern margin with relatively higher NDCI values, would have been reflected in prolonged water retention time, favoring the accumulation and growth of cyanobacteria during summer (Paerl and Paul, 2012; Reichwaldt and Ghadouani, 2012). At the same time, wind mixing would have caused nutrient (P) desorption from the lagoon bottom (Baumgarten et al., 2001), fueling some cyanobacterial growth during summer across the middle part of PL.

In summary, we used the NDCI for tracking the cyanobacterial data in the middle part of PL, in which days before the January 10th bloom (January 5th) also showed large blooms but with smaller intensity, according to the NDCI color scale (see Figure 3). Due to the Sentinel-2 passage periodicity, only on December 31st could one observe again that the NDCI was higher near the eastern margin, and a small patch was seen on the western margin. Likewise, smaller but more extended NDCI values were observed on the previous days (December 19th, 24th, and 29th; Figure 3a-c). These findings show the potential of using satellite-derived data to provide synoptical, environmental, and biological data such as cyanobacterial blooms, which can be a threat to the local economy and environmental health conditions.

CONCLUSION

In the 2019/2020 summer, two cyanobacterial bloom events were recorded within the limnic area of PL. This summer period was drier when compared with the overall climatological data, which may have affected the residence time and allowed the development and accumulation of blooms. These blooms were fairly represented with the normalized difference chlorophyll-*a* index, showing that this tool can be considered for monitoring and managing cyanoHABs in southern Brazilian waterbodies.

We believe that the influence of river discharge (and flow rates) on bloom dynamics is associated with the residence time in the limnic part of PL. However, further studies should focus on the export rate and on the time delay between river discharge and advection of cyanobacterial biomass.

The wind force may have a more complex influence on the cyanoHAB dynamics since it may be related to cyanobacterial transport across the lagoon, and it may also be combined with water mixing and resuspension of cyanobacterial populations. This kind of study can be accomplished in further work with a 3D hydrodynamic model, which can represent the vertical mixing, which is missing in this work. Nonetheless, it seemed that weak winds were responsible for the accumulation of cyanobacterial biomass in the central parts of PL. This accumulation process can be an ecological and economic threat to human populations inhabiting PL margins. In short, monitoring and management of cyanoHABs are needed more frequently and on a yearly basis since there is no available database on the occurrence, magnitude, and frequency of cyanoHABs in Patos Lagoon.

ACKNOWLEDGMENTS

The authors would like to thank two anonymous people for sending their photographs of the accumulation of cyanobacteria on the margins of Patos Lagoon in the summer of 2019–2020. B.F. Canever is granted an M.Sc. Fellowship (CAPES) Number 88887.342873/2019-00. M.S. de Souza is granted a PNPd/MEC-CAPES Fellowship Number 88882.314596/2019-01. The authors declare no conflict of interest. This work was endorsed by the GlobalHAB/IOC-SCOR. Lastly, we gratefully thank the two reviewers that helped improve this final version of our work.

AUTHOR CONTRIBUTIONS

B.F.C.: Conceptualization; Formal Analysis; Investigation; Writing - original draft; Writing - review & editing;

M.S.S.: Conceptualization; Writing - original draft; Writing - review & editing;

E.V.K.: Methodology; Meteorological Data; Writing - review & editing;

F.L.L.: Methodology; Remote Sensing Data; Writing - review & editing;

E.H.L.F.: Supervision; Writing - review & editing;

J.S.Y.: Supervision; Project Administration; Writing - review & editing.

REFERENCES

- Abreu, P. C., Hartmann, C. & Odebrecht, C. 1995. Nutrient-rich saltwater and its influence on the phytoplankton of the Patos lagoon estuary, Southern Brazil. *Estuarine, Coastal and Shelf Science*, 40(2), 219–229. DOI: [https://doi.org/10.1016/s0272-7714\(05\)80006-x](https://doi.org/10.1016/s0272-7714(05)80006-x)
- Aguilera, L., Santos, A. L. F. D. & Rosman, P. C. C. 2020. On characteristic hydraulic times through hydrodynamic modelling: discussion and application in Patos Lagoon (RS). *Ambiente e Água*, 15(2). DOI: <https://doi.org/10.4136/ambi-agua.2456>
- Andrade, M. M., Abreu, P. C., Ávila, R. A. & Möller, O. O. 2022. Importance of winds, freshwater discharge and retention time in the space-time variability of phytoplankton biomass in a shallow microtidal estuary. *Regional Studies in Marine Science*, 50, 102161. DOI: <https://doi.org/10.1016/j.rsma.2022.102161>
- Aubriot, L., Zabaleta, B., Bordet, F., Sienna, D., Risso, J., Achkar, M. & Somma, A. 2020. Assessing the origin of a massive cyanobacterial bloom in the Río de la Plata (2019): Towards an early warning system. *Water Research*, 181, 115944. DOI: <https://doi.org/10.1016/j.watres.2020.115944>
- Baumgarten, M. da G. Z., Niencheski, L. F. H. & Veeck, L. 2001. Nutrientes na coluna da água e na água intersticial de sedimentos de uma enseada rasa estuarina com aportes de origem antropica (RS-Brasil). *Atlantica (Rio Grande)*, 23, 101–116.
- Bitencourt, L. P., Fernandes, E. H., Silva, P. D. da & Möller, O. 2020. Spatio-temporal variability of suspended sediment concentrations in a shallow and turbid lagoon. *Journal of Marine Systems*, 212, 103454. DOI: <https://doi.org/10.1016/j.jmarsys.2020.103454>
- Bortolin, E. C., Weschenfelder, J., Fernandes, E. H., Bitencourt, L. P., Möller, O. O., García-Rodríguez, F. & Toldo, E. 2020. Reviewing sedimentological and hydrodynamic data of large shallow coastal lagoons for defining mud depocenters as environmental monitoring sites. *Sedimentary Geology*, 410, 105782. DOI: <https://doi.org/10.1016/j.sedgeo.2020.105782>
- Caballero, I., Fernández, R., Escalante, O. M., Mamán, L. & Navarro, G. 2020. New capabilities of Sentinel-2A/B satellites combined with in situ data for monitoring small harmful algal blooms in complex coastal waters. *Scientific Reports*, 10(1), 8743. DOI: <https://doi.org/10.1038/s41598-020-65600-1>
- Carpenter, S. R., Caraco, N. F., Corell, D. L., Howarth, R. W., Sharpey, A. N. & Smith, V. H. 1998. Nonpoint pollution of surface waters with phosphorus and nitrogen. *Ecological Applications*, 8(3), 559–568.
- Cloern, J. E. 2001. Our evolving conceptual model of the coastal eutrophication problem. *Marine Ecology Progress Series*, 210, 223–253.
- Devercelli, M. 2009. Changes in phytoplankton morpho-functional groups induced by extreme hydroclimatic events in the Middle Paraná River (Argentina). *Hydrobiologia*, 639(1), 5–19. DOI: <https://doi.org/10.1007/s10750-009-0020-6>
- Devercelli, M. & O'Farrell, I. 2013. Factors affecting the structure and maintenance of phytoplankton functional groups in a nutrient rich lowland river. *Limnologia*, 43(2), 67–78. DOI: <https://doi.org/10.1016/j.limno.2012.05.001>
- Fernandes, E. H. L., Dyer, K. R., Moller, O. O. & Niencheski, L. F. H. 2002. The Patos Lagoon hydrodynamics during an El Niño event (1998). *Continental Shelf Research*,

- 22(11–13), 1699–1713. DOI: [https://doi.org/10.1016/s0278-4343\(02\)00033-x](https://doi.org/10.1016/s0278-4343(02)00033-x)
- Ferreira, A. H. F., Minillo, A., Silva, L. de M., Yunes, J. S. 2004. Ocorrência de *Anabaena spiroides* (cianobactéria) no estuário da Lagoa dos Patos (RS, Brasil) no verão-outono de 1998. *Atlântica*, 26(1), 17–26.
- Fujita, C. C. & Odebrecht, C. 2007. Short term variability of chlorophyll a and phytoplankton composition in a shallow area of the Patos Lagoon estuary (Southern Brazil). *Atlântica*, 29(2), 93–106.
- Gorelick, N., Hancher, M., Dixon, M., Ilyushchenko, S., Thau, D. & Moore, R. 2017. Google Earth Engine: Planetary-scale geospatial analysis for everyone. *Remote Sensing of Environment*, 202, 18–27. DOI: <https://doi.org/10.1016/j.rse.2017.06.031>
- Haraguchi, L., Carstensen, J., Abreu, P. C. & Odebrecht, C. 2015. Long-term changes of the phytoplankton community and biomass in the subtropical shallow Patos Lagoon Estuary, Brazil. *Estuarine, Coastal and Shelf Science*, 162, 76–87. DOI: <https://doi.org/10.1016/j.ecss.2015.03.007>
- Ho, J. C. & Michalak, A. M. 2017. Phytoplankton blooms in Lake Erie impacted by both long-term and springtime phosphorus loading. *Journal of Great Lakes Research*, 43(3), 221–228. DOI: <https://doi.org/10.1016/j.jglr.2017.04.001>
- Kalikoski, D. C. & Vasconcellos, M. 2012. *Case study of the technical, socio-economic and environmental conditions of small-scale fisheries in the estuary of Patos Lagoon, Brazil*. Rome: FAO.
- Kennish, M. J. & Pearl, H. W. (eds.). 2010. *Coastal Lagoons: Critical Habitats of Environmental Change*. Abingdon: CRC Press.
- King, K. W., Williams, M. R. & Fausey, N. R. 2015. Contributions of Systematic Tile Drainage to Watershed-Scale Phosphorus Transport. *Journal of Environmental Quality*, 44(2), 486–494. DOI: <https://doi.org/10.2134/jeq2014.04.0149>
- Kiss, K. T. & Ács, É. 2002. Nature conservation oriented algal biodiversity monitoring investigations in the main arm and some dead arms of the River Tisza II. Phytoplankton. In: *Limnological Reports* (Vol. 34, pp. 163–171). Tulcea: International Association for Danube Research.
- Kjerfve, B. 1994. Coastal Lagoons. In: *Coastal Lagoon Process* (pp. 1–8). Amsterdam: Elsevier.
- Lehman, P. W., Boyer, G., Hall, C., Waller, S. & Gehrts, K. 2005. Distribution and toxicity of a new colonial *Microcystis aeruginosa* bloom in the San Francisco Bay Estuary, California. *Hydrobiologia*, 541(1), 87–99. DOI: <https://doi.org/10.1007/s10750-004-4670-0>
- Lobo, F. de L., Nagel, G. W., Maciel, D. A., Carvalho, L. A. S. de, Martins, V. S., Barbosa, C. C. F. & Novo, E. M. L. de M. 2021. AlgaeMAP: Algae Bloom Monitoring Application for Inland Waters in Latin America. *Remote Sensing*, 13(15), 2874. DOI: <https://doi.org/10.3390/rs13152874>
- Marreto, R. N., Baumgarten, M. da G. Z. & Wallner-Kersanach, M. 2017. Trophic quality of waters in the Patos Lagoon estuary: a comparison between its margins and the port channel located in Rio Grande, RS, Brazil. *Acta Limnologica Brasiliensia*, 29(0). DOI: <https://doi.org/10.1590/s2179-975x10716>
- Masson-Delmotte, V., Zhai, P., Pirani, A., Connors, S. L., Péan, C., Berger, S., Caud, N., Chen, Y., Goldfarb, L., Gomis, M. I., Huang, M., Leitzell, K., Lonnoy, E., Matthews, J. B. R., Maycock, T. K., Waterfield, T., Yelekçi, O., Yu, R., & Zho, B. (eds.). 2021. *Climate Change 2021: The Physical Science Basis. Contribution of Working Group I to the Sixth Assessment Report of the Intergovernmental Panel on Climate Change*. Cambridge: Cambridge University Press.
- Mendes, C. R. B., Odebrecht, C., Tavano, V. M. & Abreu, P. C. 2017. Pigment-based chemotaxonomy of phytoplankton in the Patos Lagoon estuary (Brazil) and adjacent coast. *Marine Biology Research*, 13(1), 22–35. DOI: <https://doi.org/10.1080/17451000.2016.1189082>
- Michalak, A. M., Anderson, E. J., Beletsky, D., Boland, S., Bosch, N. S., Bridgeman, T. B., Chaffin, J. D., Cho, K., Confesor, R., Daloğlu, I., DePinto, J. V., Evans, M. A., Fahnenstiel, G. L., He, L., Ho, J. C., Jenkins, L., Johengen, T. H., Kuo, K. C., LaPorte, E., Liu, X., McWilliams, M. R., Moore, M. R., Posselt, D. J., Richards, R. P., Scavia, D., Steiner, A. L., Verhamme, E., Wright, D. M. & Zagorski, M. A. 2013. Record-setting algal bloom in Lake Erie caused by agricultural and meteorological trends consistent with expected future conditions. *Proceedings of the National Academy of Sciences*, 110(16), 6448–6452. DOI: <https://doi.org/10.1073/pnas.1216006110>
- Mishra, S. & Mishra, D. R. 2012. Normalized difference chlorophyll index: A novel model for remote estimation of chlorophyll-a concentration in turbid productive waters. *Remote Sensing of Environment*, 117, 394–406. DOI: <https://doi.org/10.1016/j.rse.2011.10.016>
- Mishra, S., Stumpf, R. P., Schaeffer, B. A., Werdell, P. J., Loftin, K. A. & Meredith, A. 2019. Measurement of Cyanobacterial Bloom Magnitude using Satellite Remote Sensing. *Scientific Reports*, 9(1). DOI: <https://doi.org/10.1038/s41598-019-54453-y>
- Möller, O. O. & Castaing, P. 1999. Hydrographical Characteristics of the Estuarine Area of Patos Lagoon (30°S, Brazil). In: *Estuaries of South America* (pp. 83–100). Springer Berlin Heidelberg. DOI: https://doi.org/10.1007/978-3-642-60131-6_5
- Moller, O. O., Castaing, P., Salomon, J.-C. & Lazure, P. 2001. The Influence of Local and Non-Local Forcing Effects on the Subtidal Circulation of Patos Lagoon. *Estuaries*, 24(2), 297. DOI: <https://doi.org/10.2307/1352953>
- Möller, O. O., Castello, J. P. & Vaz, A. C. 2009. The Effect of River Discharge and Winds on the Interannual Variability of the Pink Shrimp *Farfantepenaeus paulensis* Production in Patos Lagoon. *Estuaries and Coasts*, 32(4), 787–796. DOI: <https://doi.org/10.1007/s12237-009-9168-6>
- Odebrecht, C., Abreu, P. C., Bemvenuti, C. E., Copertino, M., Muelbert, J. H., Vieira, J. P. & Seeliger, U. 2010. The Patos Lagoon estuary: Biotic responses to natural and anthropogenic impacts in the last decades (1979–2008) In: Kennish, M. J. & Paerl, H. W. (eds.). *Coastal Lagoons: Critical habitats of environmental change* (pp. 437–459). Abingdon: CRC Press.
- Odebrecht, C., Abreu, P. C., Möller, O. O., Niencheski, L. F., Proença, L. A. & Torgan, L. C. 2005. Drought effects on pelagic properties in the shallow and turbid Patos

- Lagoon, Brazil. *Estuaries*, 28(5), 675–685. DOI: <https://doi.org/10.1007/bf02732906>
- Odebrecht, C., Selliger, U., Coutinho, R. & Torgan, L. C. 1987. Florações de *Microcystis* (cianobactérias) na Lagoa dos Patos, RS. In: *Anais do simpósio sobre ecossistemas da costa sul e sudeste brasileira* (Vol. 2, pp. 280–287). Canadá: ACIESP.
- Paerl, H. W. 2017. Controlling harmful cyanobacterial blooms in a climatically more extreme world: management options and research needs. *Journal of Plankton Research*, 39(5), 763–771. DOI: <https://doi.org/10.1093/plankt/fbx042>
- Paerl, H. W., Gardner, W. S., Havens, K. E., Joyner, A. R., McCarthy, M. J., Newell, S. E., Qin, B. & Scott, J. T. 2016. Mitigating cyanobacterial harmful algal blooms in aquatic ecosystems impacted by climate change and anthropogenic nutrients. *Harmful Algae*, 54, 213–222. DOI: <https://doi.org/10.1016/j.hal.2015.09.009>
- Paerl, H. W. & Huisman, J. 2009. Climate change: a catalyst for global expansion of harmful cyanobacterial blooms. *Environmental Microbiology Reports*, 1(1), 27–37. DOI: <https://doi.org/10.1111/j.1758-2229.2008.00004.x>
- Paerl, H. W. & Otten, T. G. 2013. Harmful Cyanobacterial Blooms: Causes, Consequences, and Controls. *Microbial Ecology*, 65(4), 995–1010. DOI: <https://doi.org/10.1007/s00248-012-0159-y>
- Paerl, H. W. & Paul, V. J. 2012. Climate change: Links to global expansion of harmful cyanobacteria. *Water Research*, 46(5), 1349–1363. DOI: <https://doi.org/10.1016/j.watres.2011.08.002>
- Paerl, H. W., Yin, K. & O'Brien, T. D. 2015. SCOR Working Group 137: “Global Patterns of Phytoplankton Dynamics in Coastal Ecosystems”: An introduction to the special issue of *Estuarine, Coastal and Shelf Science*. *Estuarine, Coastal and Shelf Science*, 162, 1–3. DOI: <https://doi.org/10.1016/j.ecss.2015.07.011>
- Reichwaldt, E. S. & Ghadouani, A. 2012. Effects of rainfall patterns on toxic cyanobacterial blooms in a changing climate: Between simplistic scenarios and complex dynamics. *Water Research*, 46(5), 1372–1393. DOI: <https://doi.org/10.1016/j.watres.2011.11.052>
- Reynolds, C. S. & Davies, P. S. 2001. Sources and bioavailability of phosphorus fractions in freshwaters: a British perspective. *Biological Reviews of the Cambridge Philosophical Society*, 76(1), 27–64. DOI: <https://doi.org/10.1017/s1464793100005625>
- Seeliger, U.; Odebrecht, C.; Castello, J.P. 1998. Os Ecossistemas Costeiro e Marinho do Extremo Sul do Brasil. Rio Grande, Ecocientia. 332p.
- SEMA. 2015. Plano da Bacia Hidrográfica do Rio Camaquã. Accessed: <https://sema.rs.gov.br/030-bh-rio-camaqua>
- Sokal, R. R. & Rohlf, F. J. 1994. *Biometry: The Principles and Practice of Statistics in Biological Research* (3rd ed.). New York: W. H. Freeman.
- Song, R., Muller, J.-P., Kharbouche, S., Yin, F., Woodgate, W., Kitchen, M., Roland, M., Arriga, N., Meyer, W., Koerber, G., Bonal, D., Burbank, B., Knohl, A., Siebicke, L., Buysse, P., Loubet, B., Leonardo, M., Lerebourg, C. & Gobron, N. 2020. Validation of Space-Based Albedo Products from Upscaled Tower-Based Measurements Over Heterogeneous and Homogeneous Landscapes. *Remote Sensing*, 12(5), 833. DOI: <https://doi.org/10.3390/rs12050833>
- Souza, M. S. de, Muelbert, J. H., Costa, L. D. F., Klering, E. V. & Yunes, J. S. 2018. Environmental Variability and Cyanobacterial Blooms in a Subtropical Coastal Lagoon: Searching for a Sign of Climate Change Effects. *Frontiers in Microbiology*, 9. DOI: <https://doi.org/10.3389/fmicb.2018.01727>
- Távora, J., Fernandes, E. H., Bitencourt, L. P. & Orozco, P. M. S. 2020. El-Niño Southern Oscillation (ENSO) effects on the variability of Patos Lagoon Suspended Particulate Matter. *Regional Studies in Marine Science*, 40, 101495. DOI: <https://doi.org/10.1016/j.rsma.2020.101495>
- Thompson, P. A., O'Brien, T. D., Paerl, H. W., Peierls, B. L., Harrison, P. J. & Robb, M. 2015. Precipitation as a driver of phytoplankton ecology in coastal waters: A climatic perspective. *Estuarine, Coastal and Shelf Science*, 162, 119–129. DOI: <https://doi.org/10.1016/j.ecss.2015.04.004>
- Vaz, A. C., Junior, O. O. M. & Almeida, T. L. de. 2011. Análise quantitativa da descarga dos rios afluentes da Lagoa dos Patos. *Atlântica*, 28(1), 13–24.
- Viégas, V. R. 2021. *Mecanismos para a gestão integrada entre a bacia hidrográfica e a zona costeira: diagnóstico da sub-bacia hidrográfica do Arroio Teixeira em Tapes/RS* (mathesis). Universidade Federal do Rio Grande do Sul, Porto Alegre.
- Watanabe, F., Alcântara, E., Bernardo, N., Andrade, C. de, Gomes, A. C., Carmo, A. do, Rodrigues, T. & Rotta, L. H. 2019. Mapping the chlorophyll-a horizontal gradient in a cascading reservoirs system using MSI Sentinel-2A images. *Advances in Space Research*, 64(3), 581–590. DOI: <https://doi.org/10.1016/j.asr.2019.04.035>
- Watanabe, F., Alcântara, E., Rodrigues, T., Rotta, L., Bernardo, N., Imai, N., Sayuri, F. & Watanabe, Y. 2018. Remote sensing of the chlorophyll-a based on OLI/Landsat-8 and MSI/Sentinel-2A (Barra Bonita reservoir, Brazil). *Anais Da Academia Brasileira de Ciências*, 90(2 suppl 1), 1987–2000. DOI: <https://doi.org/10.1590/0001-3765201720170125>
- Xavier, A. C., King, C. W. & Scanlon, B. R. 2016. Daily gridded meteorological variables in Brazil (1980-2013). *International Journal of Climatology*, 36(6), 2644–2659. DOI: <https://doi.org/10.1002/joc.4518>
- Yin, F., Lewis, P., Gomez-Dans, J. & Wu, Q. 2019. Bayesian atmospheric correction over land: Sentinel-2/MSI and Landsat 8/OLI. *Geoscientific Model Development*, 15, 7933–7976. DOI: <https://doi.org/10.31223/osf.io/ps957>
- Yunes, J. S. 2009. Florações de *microcystis* na lagoa dos patos e o seu estuário: 20 Anos de Estudos. *Oecologia Australis*, 13(2), 313–318. DOI: <https://doi.org/10.4257/oeco.2009.1302.06>
- Yunes, J. S., Niencheski, L. F. H., Salomon, P. S., Parise, M., Beattie, K. A., Raggett, S. L. & Codd, G. A. 1998. Effect of nutrient balance and physical factors on blooms of toxic cyanobacteria in the Patos Lagoon, southern Brazil. *SIL Proceedings, 1922-2010*, 26(4), 1796–1800. DOI: <https://doi.org/10.1080/03680770.1995.11901048>